Sludge characteristics and membrane fouling in membrane bioreactors with various sludge retention times

Juan Xiong[a], Bo Hu[b], Cong Ma[c],*, Xingtao Zuo[b],*

[a]College of Science, Huazhong Agricultural University, Wuhan 430070, China, Tel. +86 15392879885, email: xiong@mail.hzau.edu.cn
[b]College of Resources and Environment, Huazhong Agricultural University, Wuhan 430070, China, Tel. +86 18008654775;
email: jokerhubo@hotmail.com (B. Hu), Tel. +86 15827003506; email: xingtaozuo@aliyun.com, zxt@mail.hzau.edu.cn (X.T. Zuo)
[c]State Key Laboratory of Separation Membranes and Membrane Processes, School of Environmental and Chemical Engineering,
Tianjin Polytechnic University, Tianjin 300387, China, Tel. +86 15122382805; email: hit.macong@gmail.com, macong_0805@126.com

ABSTRACT

Long-term sludge filterability and membrane fouling were investigated in a membrane bioreactor (MBR) with different sludge retention times (SRTs). The effect of SRT was evaluated systematically in terms of biomass evolution and sludge filterability such as modified fouling index (MFI) and specific cake resistance (α). The membrane fouling rate induced by the activated sludge mixed liquor in each MBR was also analyzed based on transmembrane pressure profiles and resistance-in-series model. Food to microorganism ratio gradually decreased close to 0.30 kg COD/(kg VSS d) with increasing SRT. There were no significant differences of the sludge growth rate, organic degradation rate, and the sludge yield for the MBRs. Sludge filterability significantly improved, described by the decreased MFI and α of the mixed liquor in the MBR at longer SRTs (above 20 d). The reduction of the soluble microbial products (SMP) content was relatively small as compared with a decrease in α. Lower filtration resistances were measured at SRT of 40 d coincided with lower polysaccharides and protein concentration in SMP and higher ratio of protein/polysaccharides. MBR at appropriate SRT (40 d) with a stable and high-quality permeate as well as membrane fouling mitigation could be adopted in the full-scale application.

Keywords: Sludge retention time; Sludge property; SMP; Membrane fouling

1. Introduction

Membrane bioreactor (MBR) is considered as a promising technology to achieve more stringent wastewater treatment regulations and water reuse initiatives [1]. MBR technology is seriously hampered due to the membrane fouling. Membrane fouling is mainly affected by operating conditions, solution characteristics, and membrane properties [2,3]. The successful operation of MBR wastewater treatment system depends on the decoupling of sludge residence time (SRT) from hydraulic retention time [4]. As one of the most important operational parameters, SRT controls microbial growth rate and the amount of biomass to be wasted.

Systems operated at long SRTs allow for the establishment of a more diverse microbial community with broader physiological capabilities than the bioreactors operated at low SRTs. However, longer SRT may also increase the capital and operational cost [5].

SRT affects the mixed liquor characteristics and induces changes in the physiological state of microorganisms [5,6], which would have effects on various sludge properties such as floc size, soluble microbial products (SMPs) and extracellular polymeric substances (EPSs), settling characteristics and others [7–10]. SMP and EPS are considered as the major foulants of the membrane used in MBRs [11], and they are composed of a variety of organic compounds released from

* Corresponding authors.

microorganisms due to their metabolic activity [12]. SMP has a significant effect on membrane fouling because SMP is more likely to accumulate in MBR due to membrane rejection [8]. Special importance is ascribed to carbohydrates, particularly polysaccharides in the supernatant. In most of the studies, the extended SRT led an increase in the sludge concentrations, while polysaccharides and carbohydrates fraction decreased with prolonged SRT [4,13,14], which correlated well with the variation of membrane fouling. However, other authors observed an opposite trend at prolonged SRT, membranes were fouled more severely [15], and the overall fouling resistance increased [16].

Despite the knowledge achieved in the last decades with regards to membrane technologies, the use of MBRs for treating low-strength wastewater still remains a challenge. Many controversial findings have been reported about the relationship between SRT, sludge filterability and fouling propensity. One of the possible reasons may be that only one MBR is used to study the impact of SRT by sequentially changing SRT throughout the operation. Such operation performance and the sludge characteristics could be influenced by the operation history and may not be affected solely by SRT [17]. Thus, a study on the influence of SRT on MBR applicability seemed to be an adequate option under the same conditions.

The objective of this study was to investigate the effects of SRT on sludge characteristics and membrane fouling in MBR using four parallel laboratory-scale MBRs with different SRTs. The supernatant and effluent of MBR were monitored to evaluate the effect of SMP on the performance of the reactor and evaluate the fate and inhibition of SMP. The performance of MBR was determined in terms of biomass evolution, sludge filterability, transmembrane pressure (TMP) profiles, and hydraulic resistance. Improved understanding will help to adjust the appropriate hydrodynamic conditions in the design and operation of MBRs to control membrane fouling.

2. Materials and methods

2.1. Experimental setup and operation

Four identical laboratory-scale MBRs with 22 L were continuously operated in parallel and fed with synthetic wastewater for 120 d. The composition of the synthetic wastewater is given as follows: glucose (400 mg/L), urea (33 mg/L), $(NH_4)_2SO_4$ (120 mg/L), KH_2PO_4 (15 mg/L), K_2HPO_4 (20 mg/L), $MgSO_4 \cdot 7H_2O$ (50 mg/L), $CaCl_2 \cdot 2H_2O$ (12 mg/L), $FeCl_3 \cdot 7H_2O$ (1.5 mg/L), $ZnSO_4 \cdot 7H_2O$ (0.15 mg/L), $CuSO_4 \cdot 5H_2O$ (0.05 mg/L), and $Pb(NO_3)_2$ (0.26 mg/L), and adding $NaHCO_3$ to adjust the pH value. COD fluctuated between 390 and 510 mg/L.

The inoculated activated sludge was obtained from the local municipal wastewater treatment plant, which employed the A^2/O process. The MBR process was initiated under a mixed liquor suspended solids (MLSS) concentration of 6.2 g/L. Polyvinylidene fluoride (PVDF) hollow fiber membrane with an effective area (A) of 0.3 m^2 and pore diameter of 0.22 μm was used. The oxygen concentration in the tank was measured online and controlled at 2–4 mg/L. The schematic of MBR is shown in Fig. 1. A long-term filtration operation in parallel was carried out with the filtration cycle of 10 min (8 min on and 2 min off) at a constant flux mode (10 L/(m^2h)). TMP was continuously monitored online using a high resolution (0.1 kPa) pressure sensor which was connected to a personal computer for data recording. The difference between the four MBRs was the sludge retention time (SRT) set as 10, 20, 40, and 90 d, which were named as MBR-A, MBR-B, MBR-C, and MBR-D, respectively.

2.2. Membranes cleaning

At the end of the membrane operation cycle when TMP reached to 40 kPa, the fouled membrane module was removed and washed following the procedures [18]: (i) the fouled membrane module was washed with Milli-Q water,
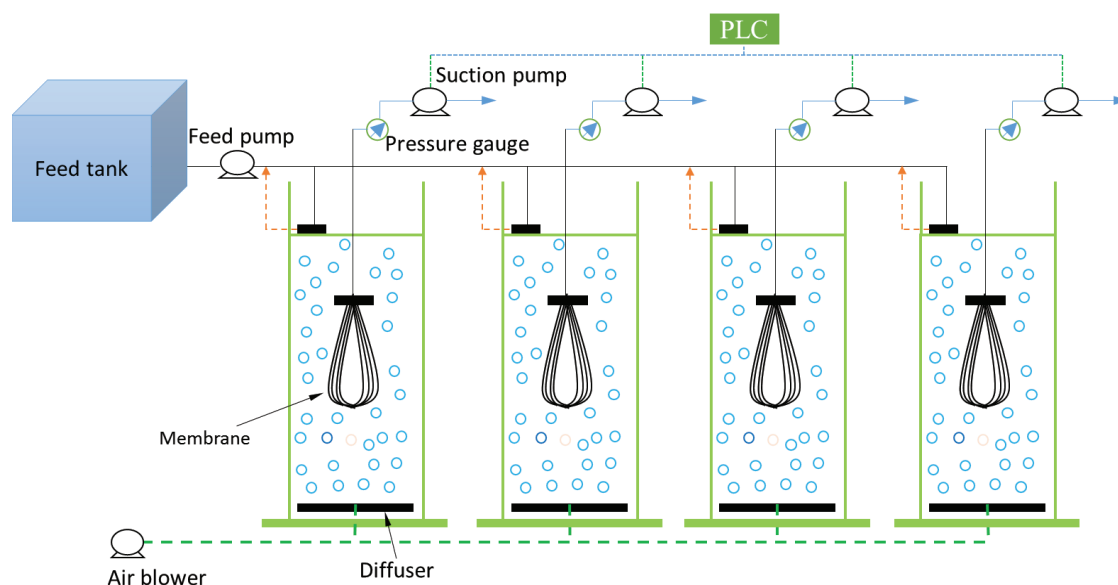
Fig. 1. Schematic diagram of MBR.

and then the foulants from the membrane surface were wiped with a sponge followed by a wash with Milli-Q water. The pure water flux of the membranes after cleaned by water was measured. (ii) After physical cleaning, the membrane was chemically cleaned by soaking in 0.01 mol/L NaOH, and then 0.1 wt% sodium citrate for 24 h, respectively. After each step of chemical cleaning, the membrane modules were rinsed completely with Milli-Q water. Then, the corresponding pure water fluxes of the membrane module were measured.

2.3. Flux recovery ratio and membrane resistance analysis

Flux recovery ratio was measured based on the pure water of the fouled and clean membranes. The resistance analysis was measured by applying resistance-in-series model to evaluate the membrane filtration characteristics [19,20].

2.4. Sludge filterability test

The filterability of MLSS and activated sludge supernatant was determined in a stirred dead-end filtration cell according to Rosenberger et al. [19]. The fouling index was obtained according to Schippers and Verdouw [20]. The sludge used for the filterability test was sampled in the later stable operation days. The batch experiment was conducted at the pressure of 10–100 kPa to examine the specific cake resistance of the sludge, collecting the data for permeate volume (*V*) as a function of time (*t*), and plotting according to the classic cake filtration Eq. (1):

$$\frac{t}{V} = \frac{\mu R}{A \Delta P} + \frac{\mu C_b \alpha}{2 A^2 \Delta P} V \tag{1}$$

where α is the specific cake resistance (m/Kg), and C_b is the concentration of suspended solid (kg/m^3). μ is the viscosity of filtrate (Pa s), and R is the filtration resistance (m^{-1}). α was obtained from the slope of the plot t/V vs. V.

2.5. Analytical methods

Chemical oxygen demand (COD), volatile suspended solids (VSS), and MLSS were measured according to the standard methods [21]. TOC was measured by Shimadzu analyzer (TOC-L cpn, Shimadzu, Japan). Polysaccharides and proteins were quantified in SMP samples filtered with 0.45-μm membrane, while SMP extraction method was reported in the literature [10]. Polysaccharides concentrations were determined spectrophotometrically with phenol sulfuric acid employing glucose as the standard [22]. Protein concentrations were determined with the Lowry method [23] using bovine serum albumin as the standard.

3. Results and discussion

3.1. COD removal

Fig. 2 showed the removal efficiencies of COD in MBRs at different SRTs. MBR-C and MBR-D had better removal efficiency under the same influent COD load. The average
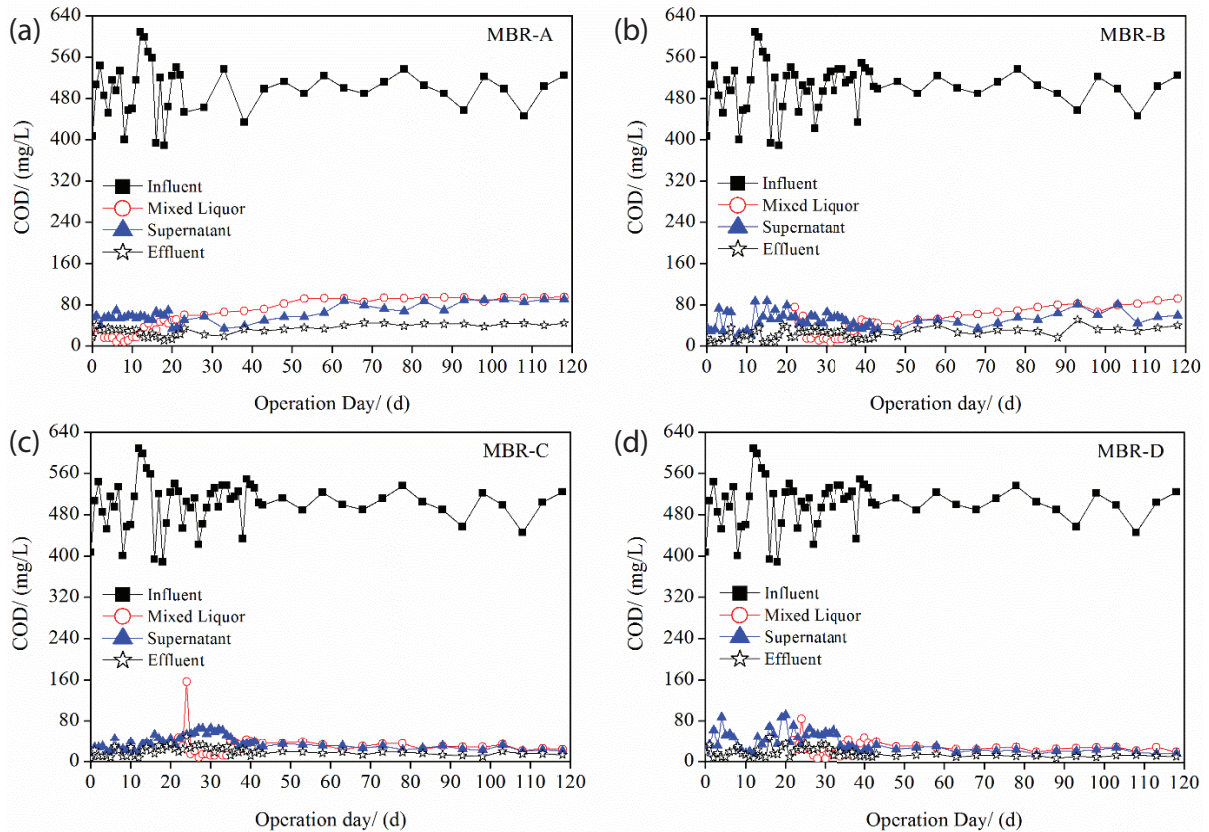
Fig. 2. Variation of COD in the MBRs at different SRT: (a) MBR-A, (b) MBR-B, (c) MBR-C, and (d) MBR-D.

effluent COD of MBR-A was 39.69 mg/L in the operation days. While the effluent COD of MBR-C and MBR-D was lower relatively. The average COD removal rates of MBR-A, B, C, and D system were 92.01%, 94.92%, 96.49%, and 96.90%, respectively. This revealed that COD removal efficiency increased and effluent quality improved with an increasing SRT, which may be attributed to the increased biomass concentration in the MBRs (Table S1).

With the SRT extended, biodegradation was the predominant effect, and the global effect was a reduction of the supernatant COD due to microbial competition for nutrients. The result followed the similar trend reported by Yurtsever et al. [6]. The difference in COD concentration between the supernatant and the effluent also indicated the occurrence of SMP accumulation due to the interception of membrane module. Part of supernatant COD was captured by the cake layers on the membrane surface, which was discussed in Section 3.7. It could be inferred that the cake layers severed as a secondary filter and enhanced the reactor effluent. COD retention rate by membranes decreased from 46.46% in MBR-A to 40.73% in MBR-C, followed by an increase of 48.11% in MBR-D. The reason for decreasing COD captured should be due to the decrement formation of the cake layers, and the membrane fouling rate decreased. Therefore, the lowest membrane fouling in MBR-C was obtained.

3.2. Biomass evolution

Fig. 3 shows the variation of MLSS and MLVSS concentration in the four MBRs. An upward trend in the evolution of MLSS and MLVSS was observed at prolong SRT (above 20 d).

Long SRT conditions implying less extracted sludge are conductive to an increase in sludge concentration. Meanwhile, MBR at prolong SRT had higher and more stable concentrations of MLSS and MLVSS (Table S1).

The average MLSS values of MBR-C and MBR-D were 6.25±0.49 and 7.66±0.68 g/L in the later 43–120 d, respectively. Their corresponding average MLVSS concentrations were 4.51±0.41 and 5.48±0.86 g/L in the MBRs at SRTs (above 20 d). The ratio of MLVSS to MLSS in all MBRs ranged from 0.72 to 0.75, which had no obvious variation with increasing SRT. Sludge volume index (SVI) of MBR-A and MBR-B increased significantly with operation time. High food to microorganism (F/M) at shortest SRT led to high SVI, resulting in poorer floc stability [24]. Whereas the SVI values of MBR-C and MBR-D were stable at 125.11 and 110.57 mL/g in the later 43–120 d, respectively, suggesting that MBR with prolonged SRT improved sludge-settling property.

The effects of the F/M ratio on the membrane filtration were also evaluated at different SRTs. At a short SRT, the F/M was high, but it gradually decreased with increasing SRT and finally approached 0.30 kg COD/(kg VSS d) (as shown in Table 1), which followed the similar trend to the result reported by Grelier et al. [25]. A low F/M ratio would cause a limiting supply of nutrient for microorganism growth, resulting in the decreased sludge activity and a low sludge yield. It is inferred that a lower F/M ratio (longer SRT) led to a reduction in membrane biofouling. These results are in accordance with results of previous studies [26,27].

According to Huang et al. [28] and Arévalo et al. [29], the sludge growth rate (R_m) and organic degradation rate ($-R_0$) were calculated and are shown in Table 1.
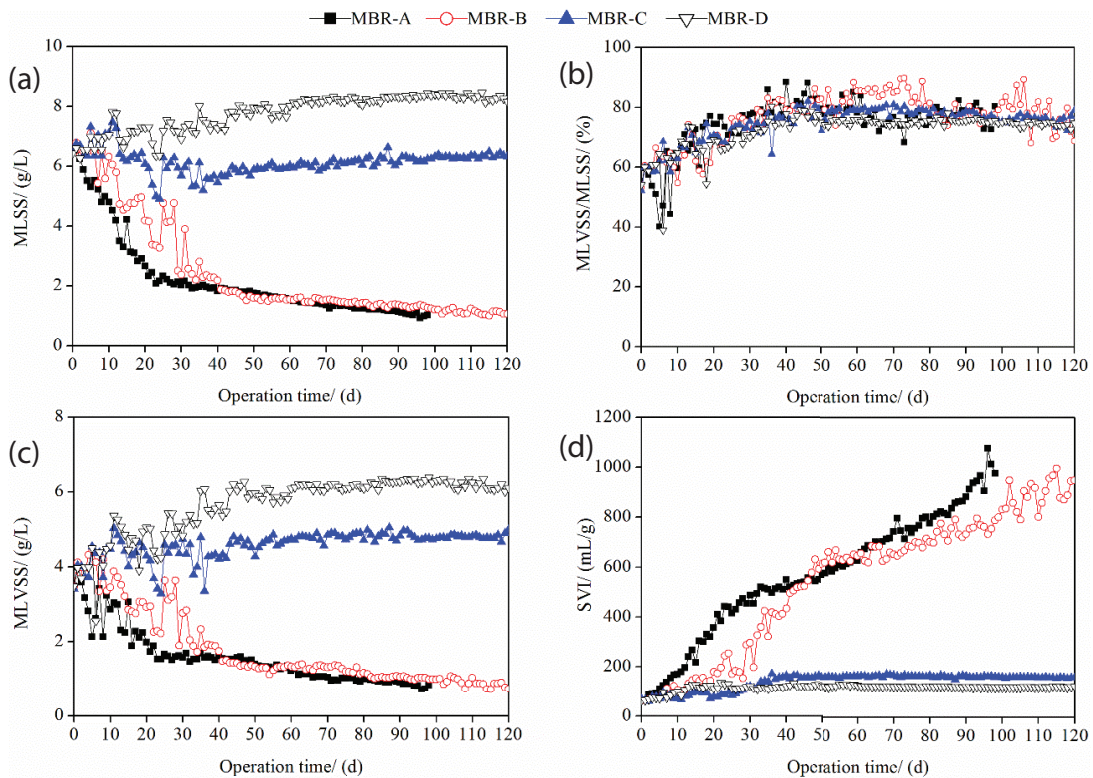
Fig. 3. Variation of (a) MLSS, (b) MLVSS/MLSS, (c) MLVSS, and (d) SVI versus time.

$$R_m = \left(\frac{dX_r}{SRT} + \frac{dX_r}{dt} \right) \qquad (2)$$

$$-R_0 = \left[\frac{C_i - C_e}{HRT} + \frac{C_i - C_s}{SRT} - \frac{C_s}{dt} \right] \qquad (3)$$

where X_r is mixed liquor VSS concentration, g VSS/L, C_i, C_s, and C_e are the influent COD, supernatant COD, and effluent COD concentration, respectively. These values are used to obtain the sludge yield (Y_{obs}, g VSS/g COD) because $Y_{obs} = R_m/-R_0$.

The sludge growth rate (R_m) increased, followed by a decrease with prolonged SRT. There were no significant differences among the organic degradation rate ($-R_0$) values. This may be explained by that with the SRT extended, microbial competition for nutrients led to the production of antibiotics, which inhibited the growth of other microorganisms, and then, a certain number of microorganisms lost their viability or died because of substrate consumption. Furthermore, owing to an increased sludge concentration at long SRT, the impeded transfer of both oxygen and substrate from the outside to the inside of activated sludge flocs was not conducive to the degradation of pollutants. However, the organic degradation rate of the incoming substrate increased slightly as SRT extended, which correlated well with the COD removal efficiency by the sludge as indicated in Fig. 1. The sludge yields (Y_{obs}) decreased from 0.12 g VSS/g COD in MBR-A to 0.07–0.10 g VSS/g COD in other MBR systems. The increase of SRT would lead to the decrease of biomass yield and the amount of excess sludge. This reflected the impact of prolonged SRT on the reduction of sludge production. In addition, Pearson coefficients revealed no linear correlation between SRT and sludge growth (*P*-value, 0.031), organic degradation rate (*P*-value, 0.73), and sludge yields (*P*-value, –0.57), respectively.

3.3. Mixed liquor filterability

In order to further understand the effect of SRT on MBR fouling, the sludge filterability was examined in filterability test using a dead-end filtration cell. The sludge was sampled from four MBRs on 90 d. The modified fouling index (MFI) suggests that the most compact fouling layers formed by the mixed liquor. As shown in Fig. 4, the MFI and specific cake resistance decreased, meaning that the fouling potential of the mixed liquor in MBRs at prolonged SRT dropped. Fig. 4(a) indicates that the MFI values for MBR-C were

ranging from 0.10×10^5 to 0.38×10^5 s/L^2, which was lower than other MBR systems under the same operation pressure. With the applied pressure, the specific cake resistance increased significantly for MBR-A with the order of magnitude 10^8, while other MBRs exhibited no significant difference as shown in Fig. 4(b). The order of magnitude for MBR-B was 10^6 and 10^4–10^5 for MBR-C and D, respectively. Lower specific resistance was observed in MBR-C.

The fouling layer formed in MBR-A had the highest compressibility (1.44) compared with other MBRs. The values were close for other MBRs, suggesting that at prolonged SRT the cohesion became weaker, a less dense fouling layer
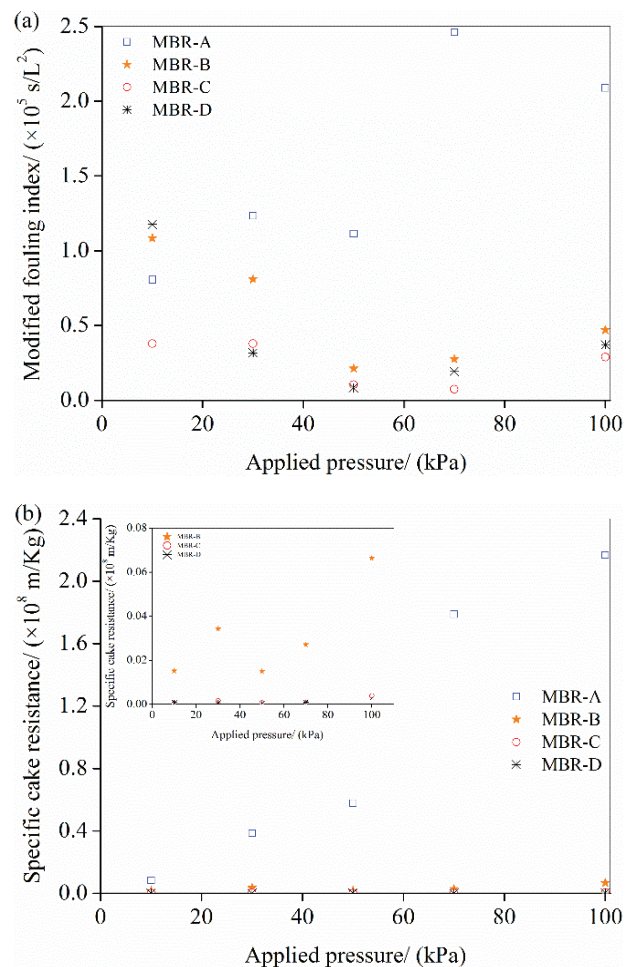
Fig. 4. MFI and specific cake resistance (α) with applied pressure: (a) MFI and (b) α.

Table 1
Sludge growth rate (R_m), organic degradation rate (R_0), and sludge yields (Y_{obs}) in the MBRs at different SRT

MBR	R_m (g VSS/(L d))	$-R_0$ (g COD/(L d))	Y_{obs} (g VSS/g COD)	F/M (kg COD/(kg VSS d))
A	0.12±0.25	1.23±0.15	0.12±0.21	1.07±0.50
B	0.19±0.06	1.29±0.10	0.07±0.18	0.89±0.45
C	0.17±0.12	1.32±0.10	0.10±0.15	0.37±0.04
D	0.15±0.08	1.32±0.10	0.07±0.13	0.32±0.06

Note: Data are expressed as mean ±SD (*n* = 32).

was observed with lower specific cake resistance and slightly higher compressibility [30].

Also, Fig. 5 shows that the fouling propensity of sludge decreased as SRT extended, expressed as the fouling resistance (R_t) produced when the mixed liquor was filtered. The resistance exerted by activated sludge was kept within a narrow range, 10^{14}–10^{15} for MBR-A, 10^{13}–10^{14} for MBR-B and MBR-D, and 10^{12}–10^{13} for MBR-C, respectively (Fig. S1). The lowest fouling potential determined by sludge filterability was observed for MBR-C, which was consistent with the corresponding TMP profiles and SMP content in the MBRs.

3.4. SMP (protein, polysaccharide, and protein/polysaccharide)

Considering that the SMP characteristics depend on operating conditions, the optimum condition for prevention and control of membrane fouling of MBR can be assumed that SMP with less fouling potential [31]. Fig. 6 presents the SMP concentration in the MBRs.

The concentrations of polysaccharides and proteins in the supernatant were always higher than those in the effluent. This indicated that polysaccharides and proteins were accumulated in the MBRs. The concentrations of polysaccharides and proteins in the supernatant and effluent were found to decrease at MBR-C and MBR-D. The fouling rate of SMP was

positively correlated with the polysaccharides content [32], suggesting MBR-C and MBR-D had a lower fouling potential, which was reconfirmed by TMP profiles that would be discussed in the following section. It is reported that the SMP in MBR with shorter SRT had relatively high polysaccharide content than at SRTs of 40 and 60 d [16]. However, Chao and Keinath [33] observed that the polysaccharide content increased with an increase in SRT.

It is clear that protein was the dominant component of the SMP in all the MBRs as indicated in Fig. 6(c). Due to their hydrophobicity and surface charge [32,34], the affinity between proteins and foulants was generally greater than that between polysaccharides and flocs. This effect mainly originated from proteins, and the effect of polysaccharides may be negligible [35]. Relative high protein/polysaccharide (P/C) ratio in MBR-C and MBR-D improved settleability due
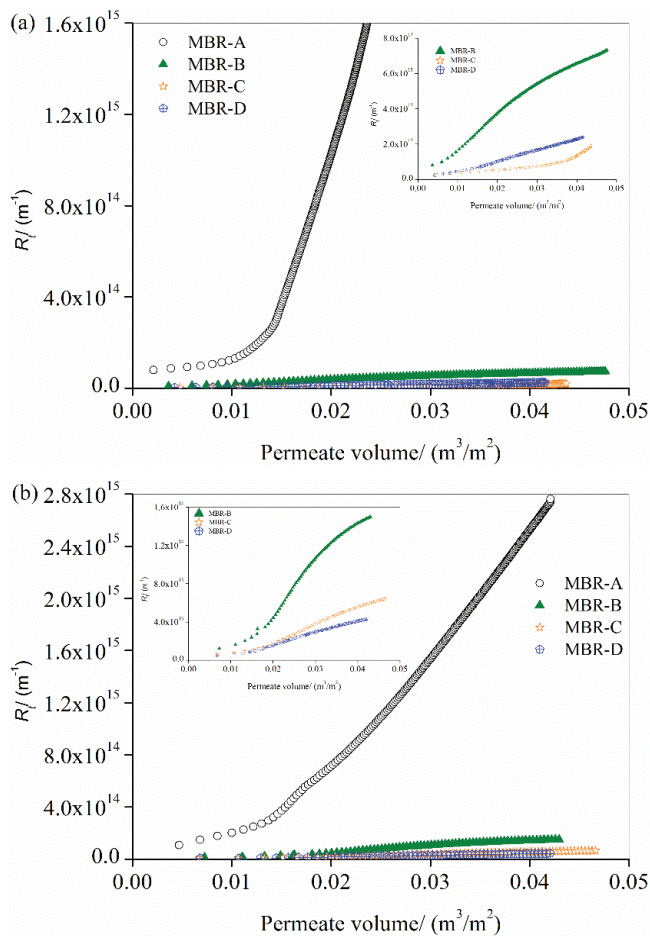
Fig. 5. Effect of SRT on sludge filterability: (a) 10 kPa and (b) 30 kPa.
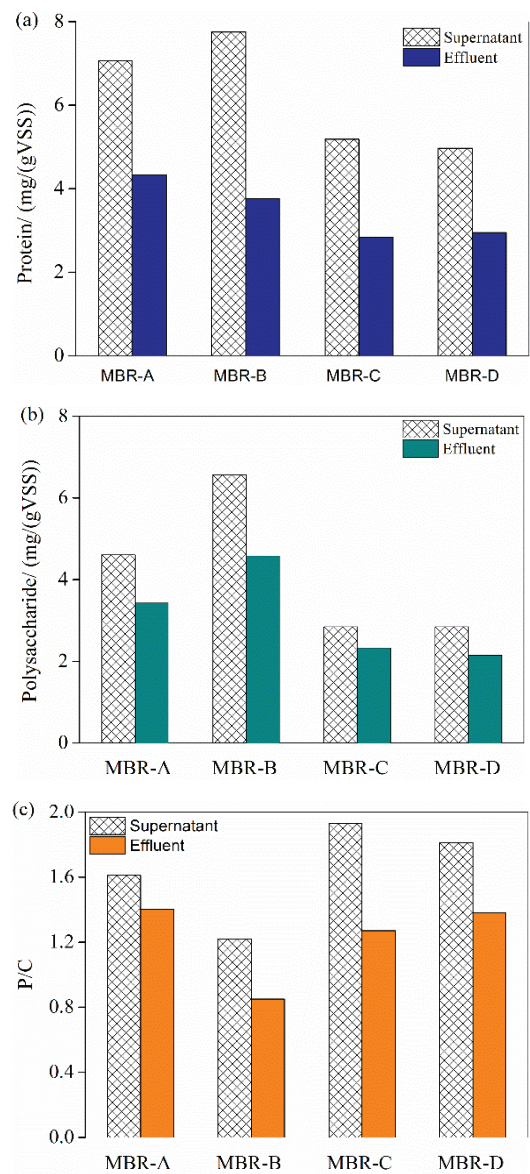
Fig. 6. (a) Protein in SMP, (b) polysaccharide in SMP, and (c) P/C ratio in SMP.

to hydrophobic nature of protein, which was consistent with the corresponding lower SVI.

From the perspective of organic matter removal in bioreactor, the viability of microorganisms and the accumulation or biodegradation of SMP, a moderate SRT could be estimated by these phenomena.

3.5. TMP profiles

TMP is a significant parameter for MBR fouling prediction [19]. The time required for TMP to rise to 40 kPa at different SRTs is shown in Fig. 7. During 120 operation days, 3.5 operation cycles were observed for MBR-B and MBR-D, but 2 cycles for MBR-C. The membrane module in MBR-A may be ruptured slightly in the second cycle due to membrane cleaning, and its corresponding TMP data could not be considered in the context.

The time approaching 40 kPa in the first cycle was 31, 46, 82, and 45 d for the MBRs, respectively. The significant

improvement in filterability by extending the filtration time as SRT increased, especially for MBR-C. TMP monitoring of TMP in the MBRs provided further evidence that membrane fouling at prolonged SRT was mitigated. The time needed for 40 kPa in the second cycle was shorter than that in the first cycle, which determined that the irreversible membrane fouling is formed. It is inferred that because all the MBR systems were operated under similar feed, SRT was mainly responsible for the improved filtration performance in the MBR by modifying the sludge characteristics of the bulk phase and the cake layer on the membrane surface.

In order to better understand the fouling rate of the MBR systems, the membrane fouling rate K was obtained as $\Delta TMP/\Delta t$. The TMP profiles seemed to exhibit two stages of fouling, the rapid increase followed by a steep TMP rise. The two phases of the K values in the cycles are listed in Table 2. The K_1 values for all the MBR systems were less than K_2, suggesting that the fouling rate in the later stage of each cycle was higher than that in the early stage. Especially, the fouling
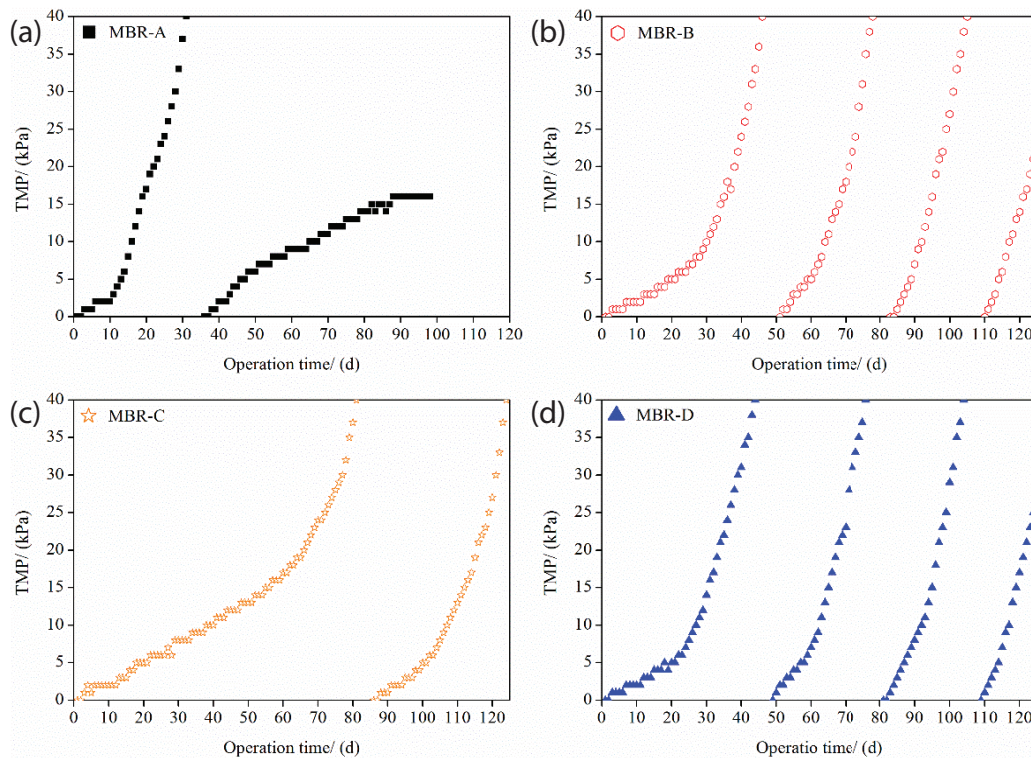
Fig. 7. TMP variation in the MBRs: (a) MBR-A, (b) MBR-B, (c) MBR-C, and (d) MBR-D.

Table 2
Fouling rate of operation cycles in the MBRs

MBR	First cycle			Second cycle			Third cycle		
	K_1 (kPa/d)	K_2 (kPa/d)	K (kPa/d)	K_1 (kPa/d)	K_2 (kPa/d)	K (kPa/d)	K_1 (kPa/d)	K_2 (kPa/d)	K (kPa/d)
A	0.248	1.646	1.295	–	–	–	–	–	–
B	0.272	2.245	0.714	0.615	3.048	1.430	0.893	2.357	2.008
C	0.271	2.257	0.379	0.349	2.893	0.909	–	–	–
D	0.253	1.885	0.854	0.566	2.500	1.451	0.967	2.764	1.720

Note: K_1, slow phase; K_2, rapid phase; and K, average value.

rates of slow phase in the first cycle were similar among all the MBRs with different SRT. Meanwhile, the K values of MBR-C were the smallest one among the four MBRs, which indicated that MBR-C suffered a slight membrane fouling due to the MBR-C system with lower protein and polysaccharide concentration, though the polysaccharide caused significant effect on the irreversible fouling.

3.6. Flux recovery and resistance analysis

The fouled membrane cleaned when TMP approached 40 kPa, and the pure water fluxes of each cycle were obtained and are showed in Table 3. At each cycle, MBR systems had similar pure water flux recovery after the same cleaning process. The flux recovery ratio decreased with the operation time, determining the membrane fouling increased, which may be explained by the irreversible fouling.

The major fouling contributor was the cake resistance as indicated in Table 4, having the much higher value compared with membrane and pore-blocking resistance. Thus,

Table 3
Pure water flux recovery of fouled membrane cleaned by different method at each cycle

Cycle	Cleaning	Pure water flux recovery (%)			
		MBR-A	MBR-B	MBR-C	MBR-D
1	Water	87.54	81.91	79.70	82.39
	Alkaline	96.15	93.97	93.28	94.33
	Acid	98.62	98.68	97.61	98.66
2	Water	–	78.53	77.01	79.25
	Alkaline	–	87.35	88.36	88.21
	Acid	–	92.35	90.90	92.39
3	Water	–	74.41	–	74.93
	Alkaline	–	82.79	–	83.73
	Acid	–	85.88	–	85.52

the reductions of the total resistance for all the MBR with increased SRT were due to the decrease in cake resistance. The polysaccharide concentration in SMP played an important role in the formation of the fouling layer. The cake resistance can be physically removed and is usually due to the deposition of large particles such as sludge floc. Hence, the total fouling resistance was more or less a function of the cake resistance.

The resistance results at the end of the different operation cycles are also listed in Table 4. The total resistance increased and became closer to each other with operation time for all the MBR systems. The irreversible resistance almost doubled, which increased from 0.6–0.7×10^{12} to 0.13×10^{13} m^{-1}. The polysaccharides in SMP are more likely to cause membrane fouling than proteins, and they were responsible for the evolution of irreversible fouling [20,36]. However, the cake resistance increased compared with the first cycle. Meanwhile, the R_c/R_t decreased and R_f/R_t increased with operation time. This can be explained by the increased irreversible fouling potential due to the foulants that hard to be cleaned increased during the longer operation

It should be noted that R_f/R_t ratio for MBR-C at the second period was higher than others, which may be due to the twofold operation time. It was also found that the R_f/R_t increased at prolonged SRT, and the values were close for MBR-B and MBR-D. The total filtration resistance and cake resistance of the mixed liquor in MBR-C had the minimum values.

3.7. Microscopic characterization of fouled membranes (EDS-FTIR)

The data obtained from energy-dispersive spectrometer (EDS) of the elements of the virgin and fouled membranes were investigated, and the results are shown in Fig. 8.

Fluorine as a base indicator of the membrane material PVDF was found to be decreased or diminished in both MBR-A, MBR-C, and MBR-D membranes, indicating the formation of cake foulants on the surface covering the whole

Table 4
Filtration resistance of different cycles in MBR at different SRT

Cycle	Resistance	MBR-A	MBR-B	MBR-C	MBR-D
1	Total resistance (R_t, 10^{13} m^{-1})	1.50	1.47	1.32	1.40
	Cake resistance (R_c, 10^{13} m^{-1})	1.40	1.36	1.21	1.30
	Irreversible fouling resistance (R_f, 10^{13} m^{-1})	0.06	0.07	0.07	0.06
	R_c/R_t (%)	93.26	92.85	91.53	92.70
	R_f/R_{tb} (%)	4.07	4.49	5.52	4.44
2	Total resistance (R_t, 10^{13} m^{-1})	–	1.53	1.39	1.49
	Cake resistance (R_c, 10^{13} m^{-1})	–	1.40	1.26	1.36
	Irreversible fouling resistance (R_f, 10^{13} m^{-1})	–	0.09	0.09	0.09
	R_c/R_t (%)	–	91.69	90.72	91.58
	R_f/R_t (%)	–	5.76	6.40	5.72
3	Total resistance (R_t, 10^{13} m^{-1})	–	1.55	–	1.54
	Cake resistance (R_c, 10^{13} m^{-1})	–	1.38	–	1.37
	Irreversible fouling resistance (R_f, 10^{13} m^{-1})	–	0.13	–	0.13
	R_c/R_t (%)	–	88.92	–	89.16
	R_f/R_t (%)	–	8.56	–	8.24

Fig. 8. Elemental content of the surafce of the virgin and fouled membrane for the MBRs.

membrane area. The highest atomic C value was obtained on the membrane of MBR-C and MBR-D mainly due to SMP adsorbed on the membrane surface. Various other elements were found on the membrane surface of MBRs compared with that of the virgin membrane, which were attributed to the presence of foulants on the surface. Higher ratio was obtained for MBR-B and MBR-D membrane, which signified more fouling occurred on such surface directly.

To verify the membrane surface chemistry changes, Fourier transform infrared (FTIR) analysis of the fouled membranes and the virgin membrane was conducted. Compared with virgin membrane (Fig. S2), the peak at 1,520–1,550 cm^{-1} was attributed to the secondary amides (CNH band, protein secondary structures) with nitroso (N=O). The peak at 1,620–1,650 cm^{-1} was the stretching of C=O and C–N amide I attributed to the presence of primary amines. The peak at 1,020 cm^{-1} was polysaccharide substance. The peak at 873 cm^{-1} was possibly due to calcit [32]. The peak at 3,674 cm^{-1} disappeared in all MBR systems, and 2,360 cm^{-1} disappeared in MBR-D, indicating that it had been fouled by protein-like and polysaccharides.

To better understand the foulants in the cake layers on the membrane surface, the extraction from the cake layers was also analyzed by FTIR. The peak stretches at wavenumbers of 3,464–3,389 and 1,467–1,412 cm^{-1}, 1,693–1,651, 1,191–1,063, and 881–588 cm^{1} confirmed the existence of the humics, protein, polysaccharides, and aromatics in the cake layers as shown in Fig. 9(b).

4. Conclusions

Sludge filterability and membrane fouling were examined at different SRT. MFI and specific cake resistance decreased with the increase of SRT. The concentration of polysaccharides and protein in SMP also decreased, which correlated with the sludge filterability. The TMP profiles and resistance-in-series determined membrane fouling propensity mitigated with extended SRT, and the formed cake layer was the major fouling contributor. MBR operated at an optimum prolonged SRT (40 d) could provide a stable and high-quality permeate, together with reasonable filtration resistances. This work shows the MBR performance systematically that is conducive to choose the best operating conditions and decrease operation cost.
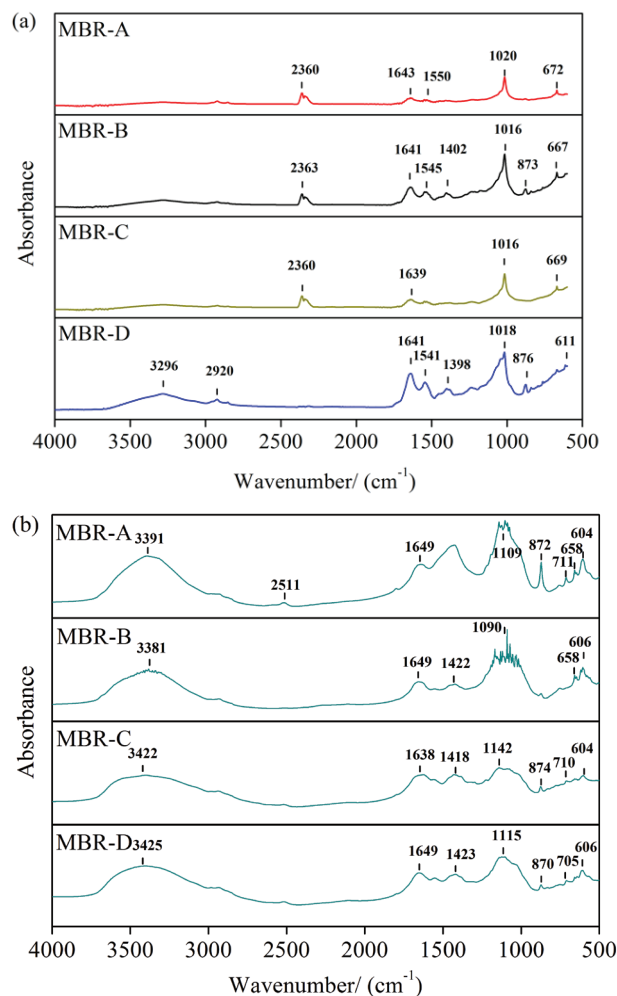
Fig. 9. FTIR spectra of (a) fouled membrane extracted from the membrane module at the end of operation cycle and (b) foulants obtained from the cake layers.

References

[1] F. Wang, B. Gao, D. Ma, R. Li, S. Sun, Q. Yue, Y. Wang, Q. Li, Effects of operating conditions on trihalomethanes formation and speciation during chloramination in reclaimed water, Environ. Sci. Pollut. Res., 23 (2016) 1576–1583.

[2] F. Meng, S. Zhang, Y. Oh, Z. Zhou, H.S. Shin, S.R. Chae, Fouling in membrane bioreactors: an updated review, Water Res., 114 (2017) 151–180.

[3] F. Schmitt, K.U. Do, Prediction of membrane fouling using artificial neural networks for wastewater treated by membrane

bioreactor technologies: bottlenecks and possibilities, Environ. Sci. Pollut. Res., 24 (2017) 22885–22913.

[4] E.B. Estrada-Arriaga, P.N. Mijaylova, Influence of operational parameters (sludge retention time and hydraulic residence time) on the removal of estrogens by membrane bioreactor, Environ. Sci. Pollut. Res., 18 (2011) 1121–1128.

[5] D. Arslan, K.J.J. Steinbusch, L. Diels, H.V.M. Hamelers, D.P.B.T.B. Strik, C.J.N. Buisman, H. De Wever, Selective short-chain carboxylates production: a review of control mechanisms to direct mixed culture fermentations, Crit. Rev. Environ. Sci. Technol., 46 (2016) 592–634.

[6] A. Yurtsever, B. Calimlioglu, E. Sahinkaya, Impact of SRT on the efficiency and microbial community of sequential anaerobic and aerobic membrane bioreactors for the treatment of textile industry wastewater, Chem. Eng. J., 314 (2017) 378–387.

[7] R. Campo, M. Capodici, G. Di Bella, M. Torregrossa, The role of EPS in the foaming and fouling for a MBR operated in intermittent aeration conditions, Biochem. Eng. J., 118 (2017) 41–52.

[8] E. Amanatidou, G. Samiotis, E. Trikoilidou, G. Pekridis, N. Taousanidis, Evaluating sedimentation problems in activated sludge treatment plants operating at complete sludge retention time, Water Res., 69 (2015) 20–29.

[9] G. Sabia, M. Ferraris, A. Spagni, Effect of solid retention time on sludge filterability and biomass activity: long-term experiment on a pilot-scale membrane bioreactor treating municipal wastewater, Chem. Eng. J., 221 (2013) 176–184.

[10] D.J. Barker, D.C. Stuckey, A review of soluble microbial products (SMP) in wastewater treatment systems, Water Res., 33 (1999) 3063–3082.

[11] B. Dong, S. Jiang, Characteristics and behaviors of soluble microbial products in sequencing batch membrane bioreactors at various sludge retention times, Desalination, 243 (2009) 240–250.

[12] K. Chen, X. Wang, X. Li, J. Qian, X. Xiao, Impacts of sludge retention time on the performance of submerged membrane bioreactor with the addition of calcium ion, Sep. Purif. Technol., 82 (2011) 148–155.

[13] Y. Kaya, G. Ersan, I. Vergili, Z.B. Gönder, G. Yilmaz, N. Dizge, C. Aydiner, The treatment of pharmaceutical wastewater using in a submerged membrane bioreactor under different sludge retention times, J. Membr. Sci., 442 (2013) 72–82.

[14] W. Lee, S. Kang, H. Shin, Sludge characteristics and their contribution to microfiltration in submerged membrane bioreactors, J. Membr. Sci., 216 (2003) 217–227.

[15] K. Ouyang, J. Liu, Effect of sludge retention time on sludge characteristics and membrane fouling of membrane bioreactor, J. Environ. Sci., 21 (2009) 1329–1335.

[16] M.M.T. Khan, S. Takizawa, Z. Lewandowski, W.L. Jones, A.K. Camper, H. Katayama, F. Kurisu, S. Ohgaki, Membrane fouling due to dynamic particle size changes in the aerated hybrid PAC-MF system, J. Membr. Sci., 371 (2011) 99–107.

[17] Y.C. Woo, J.J. Lee, W.G. Shim, H.K. Shon, L.D. Tijing, M. Yao, H.S. Kim, Effect of powdered activated carbon on integrated submerged membrane bioreactor-nanofiltration process for wastewater reclamation, Bioresour. Technol., 210 (2016) 18–25.

[18] C.A. Ng, D. Sun, M.J.K. Bashir, S.H. Wai, L.Y. Wong, H. Nisar, B. Wu, A.G. Fane, Optimization of membrane bioreactors by the addition of powdered activated carbon, Bioresour. Technol., 138 (2013) 38–47.

[19] S. Rosenberger, C. Laabs, B. Lesjean, R. Gnirss, G. Amy, M. Jekel, J.C. Schrotter, Impact of colloidal and soluble organic material on membrane performance in membrane bioreactors for municipal wastewater treatment, Water Res., 40 (2006) 710–720.

[20] J.C. Schippers, J. Verdouw, The modified fouling index, a method of determining the fouling characteristics of water, Desalination, 32 (1980) 137–148.

[21] APHA, Standard Methods for the Examination of Water and Wastewater, 20th ed., American Public Health Association, Washington, D.C., USA, 1998.

[22] M. Dubois, K.A. Gilles, J.K. Hamilton, P.A. Rebers, F. Smith, Colorimetric method for determination of sugars and related substances, Anal. Chem., 28 (1956) 350–356.

[23] O.H. Lowry, N.J. Rosebrough, A.L. Farr, R.J. Randall, Protein measurement with the Folin phenol reagent, J. Biol. Chem., 193 (1951) 265–275.

[24] L. Duan, Y. Song, H. Yu, S. Xia, S.W. Hermanowicz, The effect of solids retention times on the characterization of extracellular polymeric substances and soluble microbial products in a submerged membrane bioreactor, Bioresour. Technol., 163 (2014) 395–398.

[25] P. Grelier, S. Rosenberger, A. Tazi-Pain, Influence of sludge retention time on membrane bioreactor hydraulic performance, Desalination, 192 (2006) 10–17.

[26] Z. Ahmed, J. Cho, B.R. Lim, K.G. Song, K.H. Ahn, Effects of sludge retention time on membrane fouling and microbial community structure in a membrane bioreactor, J. Membr. Sci., 287 (2007) 211–218.

[27] J. Cho, K.G. Song, K.H. Ahn, The activated sludge and microbial substances influences on membrane fouling in submerged membrane bioreactor: unstirred batch cell test, Desalination, 183 (2005) 425–429.

[28] X. Huang, P. Gui, Y. Qian, Effect of sludge retention time on microbial behaviour in a submerged membrane bioreactor, Process Biochem., 36 (2001) 1001–1006.

[29] J. Arévalo, L.M. Ruiz, J. Pérez, M.A. Gómez, Effect of temperature on membrane bioreactor performance working with high hydraulic and sludge retention time, Biochem. Eng. J., 88 (2014) 42–49.

[30] Q. Xu, Y. Ye, V. Chen, X. Wen, Evaluation of fouling formation and evolution on hollow fibre membrane: effects of ageing and chemical exposure on biofoulant, Water Res., 68 (2015) 182–193.

[31] K. Kimura, T. Naruse, Y. Watanabe, Changes in characteristics of soluble microbial products in membrane bioreactors associated with different solid retention times: relation to membrane fouling, Water Res., 43 (2009) 1033–1039.

[32] Y. Satyawali, M. Balakrishnan, Effect of PAC addition on sludge properties in an MBR treating high strength wastewater, Water Res., 43 (2009) 1577–1588.

[33] A.C. Chao, T.M. Keinath, Influence of process loading intensity on sludge clarification and thickening characteristics, Water Res., 13 (1979) 1213–1223.

[34] M.M. Taimur Khan, S. Takizawa, Z. Lewandowski, M. Habibur Rahman, K. Komatsu, S.E. Nelson, F. Kurisu, A.K. Camper, H. Katayama, S. Ohgaki, Combined effects of EPS and HRT enhanced biofouling on a submerged and hybrid PAC-MF membrane bioreactor, Water Res., 47 (2013) 747–757.

[35] M.E. Ersahin, H. Ozgun, Y. Tao, J.B. van Lier, Applicability of dynamic membrane technology in anaerobic membrane bioreactors, Water Res., 48 (2014) 420–429.

[36] M. Remy, V. Potier, H. Temmink, W. Rulkens, Why low powdered activated carbon addition reduces membrane fouling in MBRs, Water Res., 44 (2010) 861–867.

Supplementary material
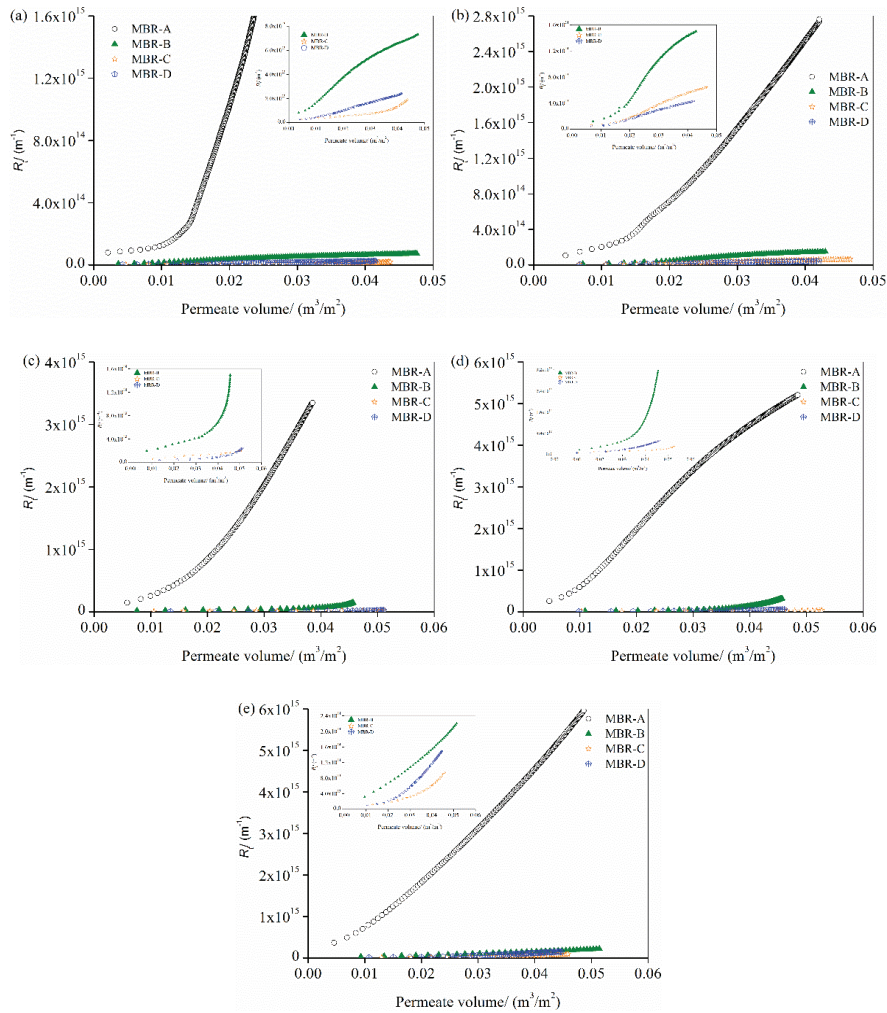
Fig. S1. Effect of SRT on sludge filterability: (a) 10 kPa, (b) 30 kPa, (c) 50 kPa, (d) 70 kPa, and (e) 100 kPa.
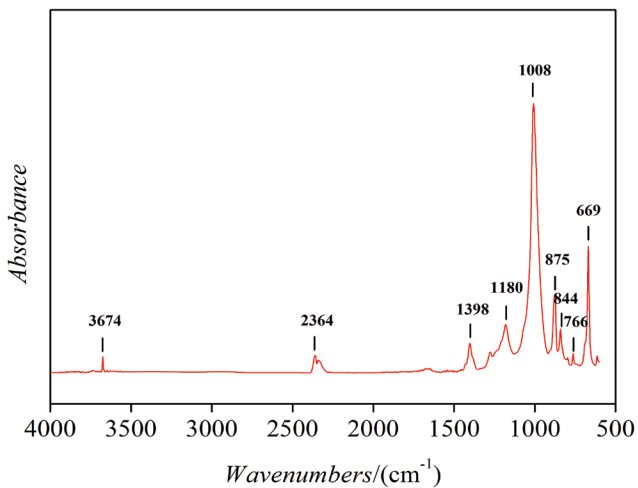
Fig. S2. FTIR spectra of the virgin membrane.

Table S1. Concentration of suspended solids in mixed liquor and F/M at different SRT

MBR	MLSS (g/L)	MLVSS (g/L)	MLSS/MLVSS
A	2.86±1.81	1.91±0.95	0.72±0.11
B	2.95±2.10	2.00±1.21	0.75±0.10
C	6.25±0.49	4.51±0.41	0.75±0.07
D	7.66±0.68	5.48±0.86	0.73±0.06